

Stepwise Deamidation of Ribonuclease A at Five Sites Determined by Top Down Mass Spectrometry[†]

Vlad Zabrouskov,^{‡,§} Xuemei Han,[‡] Ervin Welker,^{‡,||} Huili Zhai,^{‡,⊥} Cheng Lin,^{‡,*} Klaas J. van Wijk,[#] Harold A. Scheraga,[‡] and Fred W. McLafferty^{*,‡}

Department of Chemistry and Chemical Biology, Cornell University, Ithaca, New York 14853, Institute of Biochemistry, Biological Research Center of the Hungarian Academy of Science, Szeged, Hungary, and Department of Plant Biology, Cornell University, Ithaca, New York 14853

Received August 31, 2005; Revised Manuscript Received November 9, 2005

ABSTRACT: Although deamidation at asparagine and glutamine has been found in numerous studies of a variety of proteins, in almost all cases the analytical methodology that was used could detect only a single site of deamidation. For the extensively studied case of reduced bovine ribonuclease A (13 689 Da), only Asn67 deamidation has been demonstrated previously, although one study found three monodeamidated fractions. Here top down tandem mass spectrometry shows that Asn67 deamidation is extensive before Asn71 and Asn94 react; these are more than half deamidated before Asn34 reacts, and its deamidation is extensive before that at Gln74 is initiated. Except for the initial Asn67 site, these large reactivity differences correlate poorly with neighboring amino acid identities and instead indicate residual conformational effects despite the strongly denaturing media that were used; deamidation at Asn67 could enhance that at Asn71, and these enhance that at Gln74. This success in the site-specific quantitation of deamidation in a 14 kDa protein mixture, despite the minimal 1 Da ($-\text{NH}_2 \rightarrow -\text{OH}$) change in the molecular mass, is further evidence of the broad applicability of the top down MS/MS methodology for characterization of protein posttranslational modifications.

Deamidation of proteins, common both in vivo and in vitro, has been studied extensively because of its important biological effects, such as those on enzymatic activity (1–4), folding (5, 6), and proteolytic degradation (7, 8). Deamidation has also been proposed to serve as a molecular clock (9–11). However, characterization of the sites and the extent of deamidation has been a difficult analytical problem, with almost all determinations limited to the qualitative identification of a single deamidation site. Recently, top down tandem mass spectrometry (MS/MS) (12–16) has proved to be uniquely useful for kinetic studies of multicomponent protein systems (17–19). After MS separation of the target protein's molecular ions, further MS dissociation yields fragment ions whose mass shifts show which amino acids have been modified. However, deamidation has the special challenge in that its covalent $-\text{NH}_2 \rightarrow -\text{OH}$ modification

causes an only 0.984 Da mass increase, closely matching the 1.002 Da (20) spacing of the molecular ion isotope peaks (Figure 1A). Although this makes difficult the usual MS/MS isolation of product ions for their separate characterization, here top down MS/MS clearly delineates five stepwise deamidation sites in reduced bovine pancreatic ribonuclease A (RNase A,¹ $M_r = 13\,689$). Asn67, the site found here to be highly favored, is the only site previously found with certainty (2, 3, 5–7).

Rates of deamidation of asparaginyl (Asn) and glutaminyl (Gln) residues depend on protein primary sequence, three-dimensional structure, and solution parameters; increased pH and temperature and enhanced denaturation accelerate the process (11, 21–23). Deamidation of Asn is generally favored over that of Gln, in part through operation of a cyclic imide reaction mechanism that also favors the Asn67-Gly68 sequence found in RNase A (21, 22), while other neighboring residues also show an influence statistically (11, 23). However, some Asn and Gln residues are extremely resistant to in vivo deamidation (10).

In “bottom up” MS proteomics, initial digestion of the protein gives peptides whose mass spectra often provide a fast, reliable identification of the protein, but are of far less value in characterizing posttranslational modifications. In top

[†] This work was supported by Grant MCB 0090942 from the National Science Foundation to K.J.v.W. and Grants GM24893 to H.A.S. and GM16609 to F.W.M. from the National Institute of General Medical Sciences of the National Institutes of Health.

* To whom correspondence should be addressed. Phone: (607) 255-4699. Fax: (607) 255-4137. E-mail: fwm5@cornell.edu.

[‡] Department of Chemistry and Chemical Biology, Cornell University.

[§] Present address: ThermoElectron Corp., 355 River Oaks Parkway, San Jose, CA 95134.

^{||} Biological Research Center of the Hungarian Academy of Science.

[⊥] Present address: Novartis Institutes for BioMedical Research, Inc., 250 Massachusetts Ave., Cambridge, MA 02139.

[@] Present address: Boston University School of Medicine, 715 Albany St., R-806, Boston, MA 02118.

[#] Department of Plant Biology, Cornell University.

¹ Abbreviations: FT MS, Fourier transform mass spectrometry; ESI, electrospray ionization; DTT^{red}, reduced dithiothreitol; SWIFT, stored waveform inverse Fourier transform; CAD, collisionally activated dissociation; IRMPD, infrared multiphoton dissociation; ECD, electron capture dissociation; RNase A, bovine pancreatic ribonuclease A; HEPES, *N*-(2-hydroxyethyl)piperazine-*N'*-2-ethanesulfonic acid.

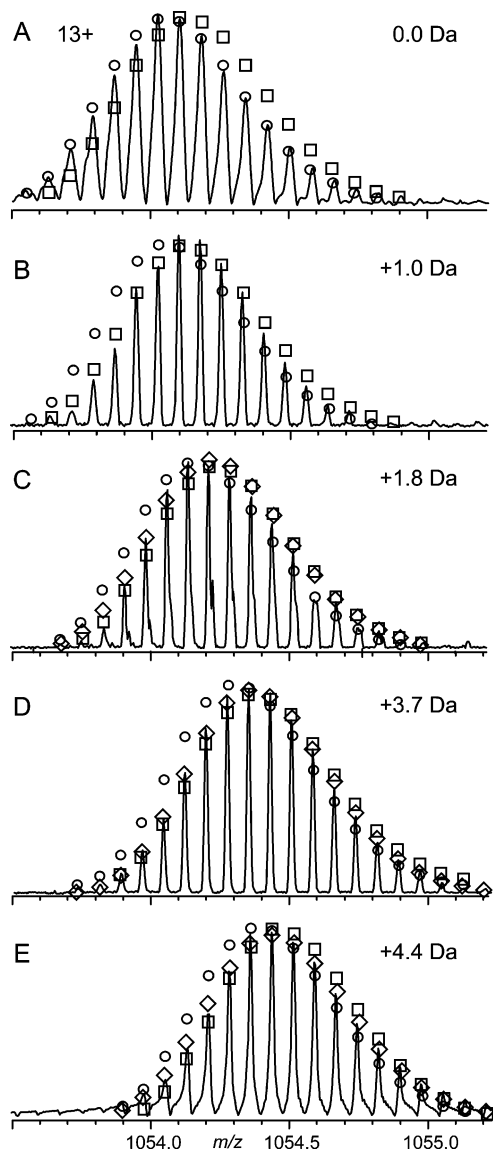


FIGURE 1: ESI spectra of RNase, 13+ molecular ions: (A) untreated and (B–E) after deamidation that caused a mass increase of 1.0, 1.8, 3.7, and 4.4 Da, respectively. (○ and □) Best fit of the theoretical abundance distribution corresponding to the protein deamidated at n and $n + 1$ sites, respectively. (◇) Best fit of the indicated fractional number of deamidations.

down MS/MS, electrospray ionization (ESI) of a protein mixture introduces their gaseous molecular ions into a Fourier transform mass spectrometer (12–19). For a specific protein, an accurate molecular mass differing from that of the gene model predicted value indicates sequence errors, alternative splicing, protein or RNA editing, and/or posttranslational modifications. These discrepancies can be identified and located by MS/MS separation and dissociation of the protein molecular ions, using methods such as collisionally activated dissociation (CAD) (24, 25), infrared multiphoton dissociation (IRMPD) (26), or electron capture dissociation (ECD) (27, 28). CAD and IRMPD cleave CO–NH bonds to produce b and y fragment ions, and ECD cleaves NH–CHR bonds to produce mainly c and z' ions. Here for reduced RNase A, these techniques establish five deamidation sites, as well their kinetic order of deamidation, that indicate extensive conformational selectivity despite the strong denaturing conditions that are employed.

EXPERIMENTAL PROCEDURES

Materials. Bovine pancreatic ribonuclease A, type XII (Sigma), was used without further purification for the deamidation experiments involving isoelectric focusing. Alternatively, RNase A was prepurified by ion-exchange chromatography on a 2.5 cm × 45 cm S-Sepharose column (Pharmacia) equilibrated with 25 mM HEPES (pH 8.0) containing 1 mM EDTA at 25 °C using a linear gradient of 0 to 150 mM NaCl over 1000 min at 2 mL/min prior to deamidation.

Deamidation. RNase A (10 mg/mL) in 0.1 M glycine/NaOH buffer (pH 9.6) containing 100 mM DTT^{red} was incubated at 78 °C, conditions chosen to accelerate the reaction. Fresh DTT^{red} was added periodically to keep the protein fully reduced. After being treated for 1 h, the protein mixture was separated on a Hydropore SCX 4.6 mm × 100 mm analytical cation-exchange HPLC column (Rainin Instrument Co.) and eluted with 25 mM HEPES (pH 7) containing 1 mM EDTA by increasing the concentration of NaCl, with the major fractions collected as samples B and C. Samples collected after treatment for 3.5 and 4.2 h were brought up to 17 mL in 7 M urea containing 30 mM DTT and 2.2% of carrier ampholytes (pI 5–8) (Bio-Rad) and the most deamidated products concentrated in a Rotofor preparative isoelectric focusing device (Bio-Rad) for 3 h at 4 °C. Fractions at pH 6.5 and 6.9 were analyzed as samples D and E.

MS Analysis. Protein samples were reduced with 20 mM DTT^{red} and desalted on a reverse-phase protein trap (Michrom Bioresources Inc.), washed with 2 mL of a 0.1:99:0.5 (v/v/v) MeCN/H₂O/CH₃COOH mixture, and eluted with 150 μL of a 50:45:5 MeCN/H₂O/CH₃COOH mixture. This eluent was loaded into a nanospray ESI emitter (2–4 μm inside diameter tip), with 1.0–1.5 kV versus the MS inlet producing a flow rate of 20–100 nL/min. The resulting ions were guided into the ion cell (10⁻⁹ Torr) of a modified 6 T Finnigan FTMS device (30). Fragmentation was achieved by plasma ECD (31) or IRMPD (26) for ions entering the FTMS cell, or by isolating specific ions in the cell using stored waveform inverse Fourier transform (SWIFT) (32) followed by CAD (25). Fragment assignments were made with THRASH (20). The mass difference (in units of 1.00235 Da) between the most abundant isotopic peak and the monoisotopic peak is denoted in italics after each M_r value.

RESULTS

The ESI mass spectrum of the 13+ molecular ions of reduced RNase A (Figure 1A) consists of a series of isotopic peaks (most abundant, 13 689.3–8 Da; calcd 13 689.3–8 Da) 1.0024 Da apart (20) whose relative intensities can be predicted (○) from the protein elemental composition. Deamidation (Figure 1B–E) produces a 0.9840 Da increase in mass (–NH₂ → –OH) for each of the isotopic peaks so that the mass spectrum of a mixture of deamidation products will have peaks at virtually identical masses, but of overlapping peak intensities. Purification by HPLC or isoelectric focusing ensured that each sample contained no more than two levels of deamidation, and the relative amounts of each that would give the observed isotopic peak intensities were calculated.

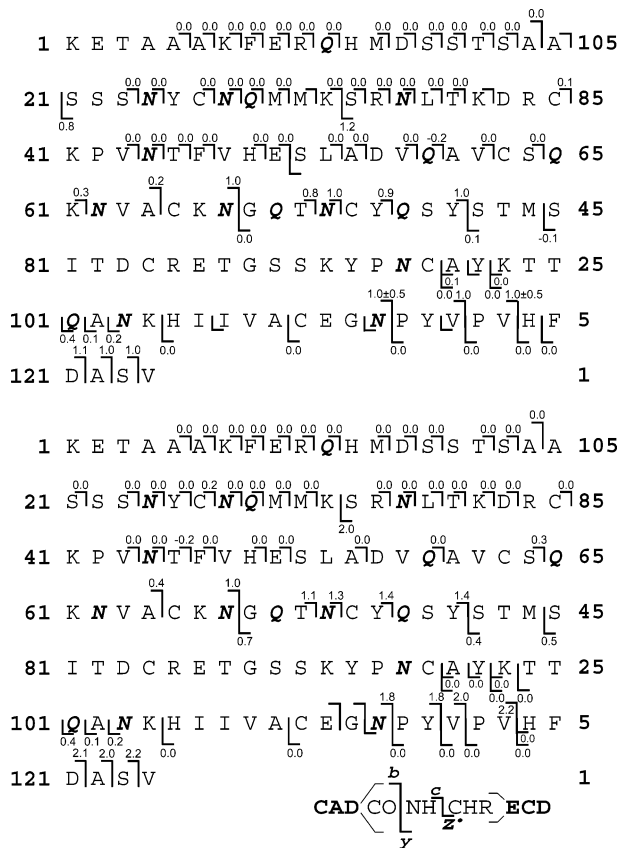


FIGURE 2: Deamidation values at specific residues for samples of (top) 1.0 and (bottom) 1.8 deamidations using cleavage assignments (as designated at the bottom) from ECD, CAD, and IRMPD spectra of RNase molecular ions. Values on each fragmentation symbol were determined as for Figure 1.

Note that the alternative measurement of the deamidation peaks by high resolution is far more difficult than indicated by the nominal mass difference of 0.0183 Da. Each of the “isotopic” peaks of Figure 1 from each degree of deamidation is also a composite of peaks of other isotopic compositions that are also isobaric (same nominal mass). Among these peaks within the 13 689.3–8 Da “peak” of Figure 1A will be those containing $^{13}\text{C}_8^{15}\text{N}_0^{34}\text{S}_0$, $^{13}\text{C}_7^{15}\text{N}_1^{34}\text{S}_0$, and $^{13}\text{C}_6^{15}\text{N}_0^{34}\text{S}_1$ (with the other atoms as their most abundant isotopes) with relative abundances of 100, 83, and 80%, respectively, with the last two lower in mass by 0.0064 and 0.0110 Da, respectively. High resolution could have been used on small fragment peaks that have few isobaric peaks, or on RNase A synthesized from ^{13}C -, ^{15}N -, and ^{34}S -depleted precursors (19, 33).

Deconvolution of Overlapping Isotopic Distributions. RNase A was deamidated under denaturing alkaline conditions for 1, 3.5, and 4.2 h. Further separation of the 1 h sample by cation exchange gave a chromatogram with three peaks in a relative area ratio of 5:43:52. These should represent products with different numbers of deamidated residues (e.g., zero, one, and two), as each deamidation adds a negative charge to the protein. The ESI mass spectra of the last two fractions had the most abundant peak at 13 690.2–8 and 13 691.6–8 Da, respectively (Figure 1B,C; Figure 1A, 13 689.3–8 Da). The relative isotopic abundances of Figure 1B are in good agreement with the calculated abundance distribution (○) for reduced RNase A shifted by +1.0 Da

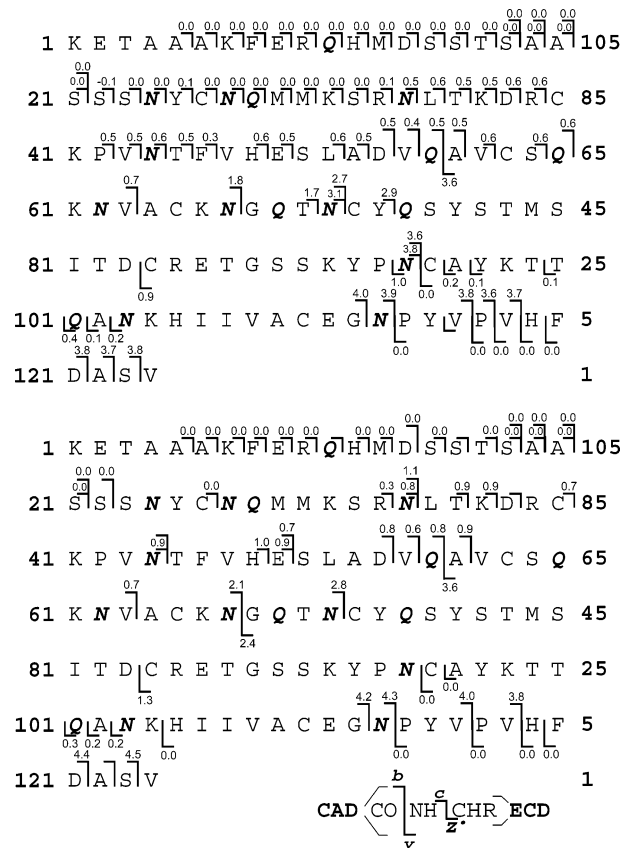


FIGURE 3: Deamidation values at specific residues for samples of (top) 3.7 and (bottom) 4.4 deamidations, as in Figure 2.

(□); therefore, most of fraction 2 is singly deamidated, consistent with the chromatographic separation. Fraction 3 gave an isotopic abundance distribution (Figure 1C) intermediate between those calculated distributions corresponding to single (○) and double (□) deamidation, while the distribution calculated for a 1:4 ratio agreed closely with experiment [Figure 1C (◇)], indicating an average of 1.8 deamidations. The 3.5 and 4.2 h deamidation products were subjected to isoelectric focusing to select the ~25 and ~15% fractions, respectively, whose mass spectra indicated that they represented more highly deamidated species. These gave overlapping isotopic distributions corresponding to 3.7 (Figure 1D) and 4.4 (Figure 1E) deamidations, respectively. Thus, the sampling times do not directly indicate the kinetic behavior, which is assumed to be exponential, and the samples will be designated by their deamidation degree: 0.0, 1.0, 1.8, 3.7, and 4.4 (Figure 1).

These overlapping molecular ions that could represent more than one degree of deamidation were then dissociated by CAD and IRMPD to produce b and y fragment ions and by ECD to produce c, z*, and y fragment ions. Their overlapping fragment peak isotopic clusters were deconvoluted as in Figure 1, with the deamidation values shown in Figures 2 and 3. The precision of these values depends on peak intensities (not shown) and increases with a decrease in mass. Plots of these values (calculated to two decimal places, Figure 4) show the increasing level of deamidation versus each of the Asn and Gln sites of RNase A for the four product samples. Besides the expected deamidation products Asp and Glu, isomers such as isoaspartic acid can also be formed (3–6). No effort was made here to differenti-

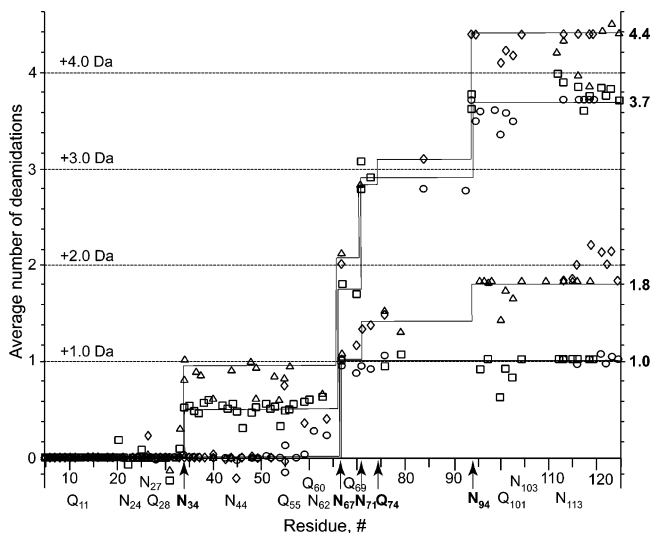


FIGURE 4: Deamidation map of the RNase A sequence from the values of Figures 2 and 3. Symbols for b or c and y or z⁺ fragment ions, respectively: 1.0 (○ and □), 1.8 (◇ and △), 3.7 (◻ and ◊), and 4.4 deamidations (△ and ◇). The deamidation value shown for a y or z⁺ (C-terminal) ion represents the difference between its observed value and that of its parent ions.

ate such products, although this was recently achieved for peptides with ECD MS (34).

DISCUSSION

Monodeamidated Fraction. For the 1 h deamidation products, the isotopic abundance distribution of the sample B molecular ions (Figure 1B) shows a mass shift (1.0) corresponding closely to the unitary deamidation expected from the cation-exchange chromatogram. MS/MS cleaved 69 of the 123 interresidue bonds (Figure 2, top), with nearly all fragments containing zero or one deamidation, within experimental error. For the fragment ions containing the N-terminus (b and c), all with 60 amino acids or fewer exhibit deamidation values close to 0.0, while all with 67 or more exhibit values of ~ 1.0 . Except for the c_{61} and b_{64} values, this restricts the site to Asn67, an assignment consistent with most previous ion studies of RNase A (3–5, 7). In support, the C-terminal y and z⁺ ions with 57 residues (Asn67–Gly68 bond cleavage) or fewer have deamidation values of ~ 0.0 , while those with 75 or more have values of ~ 1.0 . The c_{61} value of 0.3 (possible deamidation at Gln60) and the b_{64} value of 0.2 (Gln60 and/or Asn62) have not increased appreciably in the dideamidated sample C spectrum [Figures 2 (bottom) and 4]; therefore, the corresponding values of Figure 2 (top) should represent an unidentified interference or noise. Under our conditions, Asn67 is not only the first residue in RNase A to deamidate; this is nearly complete in 1 h (0:1:2 deamidations at a 5:43:52 ratio), with $<10\%$ monodeamidation at other sites. The three monodeamidated fractions separated previously (2, 29) apparently were isomeric Asn67 deamidates.

Dideamidated Fraction. Sample C of 1.8 deamidations yields (Figure 2, bottom) seven N-terminal fragment ions b_{113} or larger that have 1.8–2.2 deamidations, showing that this cation-exchange fraction is dominated by dideamidated products. As shown also by Figure 4, this additional deamidation is on the C-terminal side of Asn67, and the values of ~ 0.0 for C-terminal fragment ions as large as 29

residues show that deamidation has not occurred above Asn94. The complementary c_{76} and y_{48} fragments have a cumulative deamidation of $1.4 + 0.4 (=1.8)$ so that the next deamidation is occurring competitively on both sides of the position 76 bond. Asn94 is the only possibility on the C-terminal side. The 1.1, 1.3, 1.4, and 1.4 values for the c_{70} , c_{71} , c_{73} , and c_{76} fragments, respectively, indicate substantial deamidation at Asn71; the possible assignment of Gln69 is not supported by the 3.7 deamidation sample data, *vide infra*. Thus, the far slower secondary deamidations at Asn71 and Asn94 have started at approximately equivalent rates within 1 h, possibly with their rates increased by deamidation at Asn67.

Sample with 3.7 Deamidations. For the $\sim 25\%$ fraction of the 3.5 h sample separated to give the highest extent of deamidation, MS/MS spectra [Figures 3 (top) and 4] showed that the N-terminal fragment ions with fewer than 34 residues and the C-terminal ions with fewer than 31 residues exhibit mainly 0.0 values, demonstrating that deamidation is localized between Asn34 and Asn94. Completed deamidation at the three sites (Asn67, -71, and -94) identified in the 1 h sample accounts for 3.0 of the 3.7 total deamidations, based on $b_{63} = 0.7$ ($c_{59} = b_{60} = 0.6$) and $b_{94} = 3.6$ ($c_{94} = 3.8$). Of the remaining 0.7 deamidation, ~ 0.5 corresponds to the 23 c and b fragment ions of 34–63 residues, demonstrating that now $\sim 50\%$ of Asn34 is deamidated. An early study (21) found that hydroxylamine cleaved the Asn67–Gly68 bond of RNase A with minor cleavage at the Asn34–Leu35 bond. The remaining small difference of ~ 0.2 deamidation cannot be assigned within experimental error to a specific site.

Sample with 4.4 Deamidations. MS/MS spectra of the ions from the $\sim 15\%$ most deamidated fraction of the 4.2 h product [Figures 3 (bottom) and 4] indicate that Asn34 has become almost fully (0.9) deamidated; now Asn34, -67, -71, and -94 account for 3.9 of the 4.4 total deamidations. Most of the remainder must occur at new sites after Asn71 ($b_{71} = 2.8$) and before Asn94 ($z_{29}^+ = y_{30} = 0.0$), indicating Gln74 as the new site with ~ 0.5 deamidation (although, within experimental error, minor deamidation at Asn103 is also possible).

The one site identified in previous studies, Asn67, is deamidated the most rapidly, followed by Asn71 and Asn94 at similar rates, followed by deamidation at Asn34 and finally at Gln74, with six asparagines and six glutamines unreacted. The possibility that a significant product from reaction at one of these sites was lost in separating a protein with the same number of deamidations seems remote, as this would require a significant difference in their pI values. Calculations (35) predict that proteins with the same number of deamidations, but at different sites, will have the same pI values to two decimal places, while 0–4 deamidations give values of 8.64, 8.43, 8.15, 7.70, and 7.03, respectively.

Enhanced CAD/IRMPD at Asp. For protein ions from ESI undergoing CAD and IRMPD, a 4.5 times higher, on average, probability of cleavage was found for the C-terminal side of Asp versus that of Asn (36). This possible higher N-terminal fragment yield at Asp versus Asn could erroneously inflate a partial deamidation value for that site from IRMPD or CAD, but not a true 0.0 or 1.0 value, or an ECD value. This appears to have no appreciable effect on the conclusions given above: the b_{67} fragment ion is always formed from fully deamidated Asn67, and the b_{71} and b_{94}

values of Figure 3 (top) and b_{34} of Figure 3 (bottom) are lower than the corresponding c_{71} , c_{94} , and c_{34} values.

Influence of Neighboring Residues. In earlier studies (2, 3, 7, 22), the identity of the amino acids adjacent to Asn and Gln has shown some correlation with preferential deamidation. The fastest deamidation at Asn67 has been found to occur through a cyclic imide of its -Asn-Gly-sequence (22, 23), but none of the other 16 Asn or Gln residues in RNase A are followed by a Gly residue. Although a preference has been found for the deamidation of Asn and Gln residues with a neighboring Ser or Thr (23), here there is evidence for deamidation in only half of such sequences in RNase A. Deamidation via such a neighboring nucleophile mechanism could possibly provide an explanation for the -Asn-Cys- sequences of the second and third deamidation sites, but these possible rate increases could arise from the initial Asn67 reaction (vide supra).

The reduced, denaturing conditions employed here not only accelerated the naturally slow deamidation of RNase A but also should have minimized conformational effects; RNase A reduced under similar conditions is considered to be a model for a statistical coil without residual structure (37, 38). However, the nonrandom distribution of the Asn34, Asn67, Asn71, Gln74, and Asn94 deamidation sites of the 17 possible suggests instead a nonrandom conformational distribution, as shown recently for the reduced form of RNase A under mild folding conditions (39, 40).

In summary, the top down MS/MS approach has been applied successfully to characterize deamidated isoforms of bovine ribonuclease A. Of 17 possible deamidation sites, of which only one was implicated in numerous previous studies (2, 3, 5–7, 22), five have been identified. Their rates differ substantially and are reasonably competitive at only two sites, Asn71 and Asn94, as established using a combination of CAD, IRMPD, and ECD fragmentation techniques. The success here, despite a deamidation change of only +1.0 Da, further demonstrates the applicability of this methodology to the characterization and quantitation of a wide variety of chemical modifications to proteins (17–19).

ACKNOWLEDGMENT

We are grateful to Cynthia Kinsland from the Protein Purification Facility, Department of Chemistry and Chemical Biology, for help with preparative isoelectrofocusing and to Jean-Benoit Peltier, Sabine Baumgart, Mahesh Narayan, and Kathrin Breuker for helpful discussions.

REFERENCES

- Flatmark, T., and Sletten, K. (1968) Multiple forms of cytochrome *c* in the rat, *J. Biol. Chem.* **243**, 1623–1629.
- Venkatesh, Y. P., and Vithayathil, P. J. (1984) Isolation and characterization of monodeamidated derivatives of bovine pancreatic ribonuclease A, *Int. J. Pept. Res.* **23**, 494–505.
- Di Donato, A., Ciardiello, M. A., de Nigris, M., Piccoli, R. L., Mazzarella, L., and D'Alessio, G. (1993) Selective deamidation of ribonuclease A. Isolation and characterization of the resulting isoaspartyl and aspartyl derivatives, *J. Biol. Chem.* **268**, 4745–4751.
- Solstad, T., Carvalho, R. N., Andersen, O. A., Waidelich, D., and Flatmark, T. (2003) Deamidation of labile asparagine residues in the autoregulatory sequence of human phenylalanine hydroxylase, *Eur. J. Biochem.* **270**, 929–938.
- Catanzano, F., Graziano, G., Capasso, S., and Barone, G. (1997) Thermodynamic analysis of the effect of selective monodeamidation at asparagine 67 in ribonuclease A, *Protein Sci.* **6**, 1682–1693.
- Orru, S., Vitagliano, L., Esposito, L., Mazzarella, L., Marino, G., and Ruoppolo, M. (2000) Effect of deamidation on folding of ribonuclease A, *Protein Sci.* **9**, 2577–2582.
- Thannhauser, T., and Scheraga, H. A. (1985) Reversible blocking of half-cysteine residues of proteins and an irreversible specific deamidation of asparagine-67 of S-sulforibonuclease under mild conditions, *Biochemistry* **24**, 7681–7688.
- Solstad, T., and Flatmark, T. (2000) Microheterogeneity of recombinant human phenylalanine hydroxylase as a result of nonenzymatic deamidations of labile amide containing amino acid, *Eur. J. Biochem.* **267**, 6302–6310.
- Robinson, A. B., McKerrow, J. H., and Cary, P. (1970) Controlled deamidation of peptides and proteins: An experimental hazard and a possible biological timer, *Proc. Natl. Acad. Sci. U.S.A.* **66**, 753–757.
- Takemoto, L., and Boyle, D. (2000) Specific glutamine and asparagine residues of γ -S crystallin are resistant to *in vivo* deamidation, *J. Biol. Chem.* **275**, 26109–26112.
- Robinson, N. E., and Robinson, A. B. (2001) Prediction of protein deamidation rates from primary and three-dimensional structure, *Proc. Natl. Acad. Sci. U.S.A.* **98**, 4367–4372.
- Kelleher, N. L., Lin, H. Y., Valaskovic, G. A., Aaserud, D. J., Fridriksson, E. K., and McLafferty, F. W. (1999) Top down versus bottom up protein characterization by tandem high-resolution mass spectrometry, *J. Am. Chem. Soc.* **121**, 806–812.
- McLafferty, F. W., Fridriksson, E. K., Horn, D. M., Lewis, M. A., and Zubarev, R. A. (1999) Biomolecule mass spectrometry, *Science* **21**, 1289–1290.
- Ge, Y., Lawhorn, B. G., ElNaggar, M., Strauss, E., Park, J., Begley, T. P., and McLafferty, F. W. (2002) Top down characterization of larger proteins (45 kDa) by electron capture dissociation mass spectrometry, *J. Am. Chem. Soc.* **124**, 672–678.
- Kelleher, N. L. (2004), Top-Down Proteomics, *Anal. Chem.* **76**, 196A–203A.
- Burns, K. E., Xiang, Y., Kinsland, C. L., McLafferty, F. W., and Begley, T. P. (2005) Reconstitution and Biochemical Characterization of a New Pyridoxal-5'-phosphate Biosynthetic Pathway, *J. Am. Chem. Soc.* **127**, 3682–3683.
- Narayan, M., Xu, G., Ripoli, D. R., Zhai, H., Breuker, K., Wanjalla, C., Leung, H. J., Navon, A., Welker, E., McLafferty, M. W., and Scheraga, H. A. (2004) Dissimilarity in the Reductive Unfolding Pathways of Two Ribonuclease Homologues, *J. Mol. Biol.* **338**, 795–809.
- Xu, G., Zhai, H., Narayan, M., McLafferty, M. W., and Scheraga, H. A. (2004) Simultaneous Characterization of the Reductive Unfolding Pathways of RNase B Isoforms by Top-Down Mass Spectrometry, *Chem. Biol.* **11**, 517–524.
- Zhai, H., Dorrestein, P. C., Chatterjee, A., Begley, T. P., and McLafferty, F. W. (2005) Simultaneous Kinetic Characterization of Multiple Protein Forms by Top Down Mass Spectrometry, *J. Am. Soc. Mass Spectrom.* **16**, 1052–1059.
- Horn, D. M., Zubarev, R. A., and McLafferty, F. W. (2000) Automated reduction and interpretation of high-resolution electrospray mass spectra of large molecules, *J. Am. Soc. Mass Spectrom.* **11**, 320–332.
- Bornstein, P., and Balian, G. (1970) The specific nonenzymatic cleavage of bovine ribonuclease with hydroxylamine, *J. Biol. Chem.* **245**, 4854–4856.
- Meinwald, Y. C., Stimson, E. R., and Scheraga, H. A. (1986) Deamidation of the asparaginyl-glycyl sequence, *Int. J. Pept. Protein Res.* **28**, 79–84.
- Wright, H. T. (1991) Sequence and structure determinants of the nonenzymatic deamidation of asparagine and glutamine residues in proteins, *Protein Eng.* **4**, 283–294.
- Gauthier, J. W., Trautman, T. R., and Jacobson, D. B. (1991) Sustained off-resonance irradiation for collision-activated dissociation involving Fourier transform mass spectrometry. Collision-activated dissociation technique that eliminates infrared multiphoton dissociation, *Anal. Chim. Acta* **246**, 211–225.
- Senko, M. W., Speir, J. P., and McLafferty, F. W. (1994) Collisional activation of large multiply charged ions using Fourier transform mass spectrometry, *Anal. Chem.* **66**, 2801–2808.
- Little, D. P., Speir, J. P., Senko, M. W., O'Connor, P. B., and McLafferty, F. W. (1994) Infrared multiphoton dissociation of

- large multiply charged ions for biomolecule sequencing, *Anal. Chem.* **66**, 2809–2815.
27. Zubarev, R. A., Kelleher, N. L., and McLafferty, F. W. (1998) Electron capture dissociation of multiply charged protein cations. A nonergodic process, *J. Am. Chem. Soc.* **120**, 3265–3266.
 28. Zubarev, R. A., Horn, D. M., Fridriksson, E. K., Kelleher, N. L., Kruger, N. A., Lewis, M. A., Carpenter, B. K., and McLafferty, F. W. (2000) Electron capture dissociation for structural characterization of multiply charged protein cations, *Anal. Chem.* **72**, 563–573.
 29. Venkatesh, Y. P., and Vithayathil, P. J. (1985) Influence of deamidation(s) in the 67–74 region of ribonuclease on its refolding, *Int. J. Pept. Res.* **25**, 27–32.
 30. Beu, S. C., Senko, M. W., Quinn, J. P., Wampler, F. M., III, and McLafferty, F. W. (1993) Fourier transform electrospray instrumentation for tandem high-resolution mass spectrometry of large molecules, *J. Am. Soc. Mass Spectrom.* **4**, 557–565.
 31. Sze, S. K., Ge, Y., Oh, H., and McLafferty, F. W. (2003) Plasma electron capture characterization of large dissociation for the proteins by top down mass spectrometry, *Anal. Chem.* **75**, 1599–1603.
 32. Wang, T. C., Ricca, T. L., and Marshall, A. G. (1986) Extension of dynamic range in Fourier transform ion cyclotron resonance mass spectrometry via stored wave form inverse Fourier transform excitation, *Anal. Chem.* **58**, 2935–2938.
 33. Marshall, A. G., Senko, M. W., Li, W., Li, M., Dillon, S., Guan, S., and Logan, T. M. (1997) Protein Molecular Weight to 1 Da by ¹³C, ¹⁵N Double-Depletion and FT-ICR Mass Spectrometry, *J. Am. Chem. Soc.* **119**, 433–434.
 34. Cournoyer, J. J., Pittman, J. L., Ivleva, V. B., Fallows, E., Waskell, L., Costello, C. E., and O'Connor, O. B. (2005) Deamidation: Differentiation of aspartyl from isoaspartyl products in peptides by electron capture dissociation, *Protein Sci.* **14**, 452–463.
 35. Bjellqvist, B., Bases, B., Olsen, E., and Celis, J. E. (1994) Reference points for comparisons of two-dimensional maps of proteins from different human cell types defined in a pH scale where isoelectric points correlate with polypeptide compositions, *Electrophoresis* **15**, 529–539.
 36. Kruger, N. A., Zubarev, R. A., Carpenter, B. K., Kelleher, N. L., Horn, D. M., and McLafferty, F. W. (1999) Electron capture versus energetic dissociation of protein ions, *Int. J. Mass Spectrom.* **182/183**, 1–5.
 37. Qi, P. X., Sosnick, T. R., and Englander, S. W. (1998) The burst phase in ribonuclease A folding and solvent dependence of the unfolded state, *Nat. Struct. Biol.* **5**, 882–884.
 38. Krantz, B. A., Mayne, L., Rumbley, J., Englander, S. W., and Sosnick, T. R. (2002) Fast and slow intermediate accumulation and the initial barrier mechanism in protein folding, *J. Mol. Biol.* **324**, 359–371.
 39. Navon, A., Ittah, V., Laity, J. H., Scheraga, H. A., Haas, E., and Gussakovsky, E. E. (2001) Local and long-range interactions in the thermal unfolding transition of bovine pancreatic ribonuclease A, *Biochemistry* **40**, 93–104.
 40. Navon, A., Ittah, V., Landsman, P., Scheraga, H. A., and Haas, E. (2001) Distributions of intramolecular distances in the reduced and denatured states of bovine pancreatic ribonuclease A. Folding initiation structures in the C-terminal portions of the reduced protein, *Biochemistry* **40**, 105–118.

BI0517584